3*p*-photoionization resonances of atomic Fe, Co, and Ni studied by the observation of singly and doubly charged photoions

H. Feist, M. Feldt, Ch. Gerth, M. Martins,* P. Sladeczek, and P. Zimmermann
Institut für Strahlungs und Kernphysik, Technische Universität Berlin, D-10623 Berlin, Germany
(Received 23 August 1995)

Using monochromatized synchrotron radiation and atomic beam technique the photoion spectra of Fe, Co, and Ni in the region of the 3*p* resonances were measured. For the interpretation of the spectra the photoionization cross sections were calculated, taking into account strong interconfiguration mixing of the type $(3d,4s)^N$ and the thermal population of the different fine-structure levels in the ground states according to the temperature of about 1800 K for the evaporation of the metals. The calculations were performed in the framework of overlapping resonances interacting with many continua. Good agreement of the main features with the experimental results were obtained. Special emphasis is given to the discussion on the origin of doubly charged photoions.

PACS number(s): 32.80 Fb, 32.80 Hd

I. INTRODUCTION

The study of the inner-shell spectra of the $3d$ metal atoms has stimulated many experimental and theoretical investigations ([1], and references within). For the theory there is the challenge of the open $3d$ shell atoms with their complex many-electron systems. For the experimentalist the technological importance of these metals and their compounds in many fields is a strong motivation.

The $3p$-photoionizataion resonances in the region of 30–80 eV, in particular, have attracted the interest of scientists. Meyer *et al.* [2] systematically investigated these resonances in absorption and photoelectron emission. They found that the majority of the observed strong resonances can be attributed to $3p$ transitions into unoccupied $3d$ orbitals $3p^6 3d^N \rightarrow 3p^5 3d^{N+1}$ with the subsequent emission of a $3d$ electron $3p^5 3d^{N+1} \rightarrow 3p^6 3d^{N-1} \varepsilon(p,f)$ as the main decay channel where both excitation and decay are governed by the large overlap of the $3p$ and $3d$ wave functions.

For a quantitative analysis one has to take into account that the coupling properties of the unfilled $3d$ shells give rise to a large number of discrete states that can interact with a correspondingly large number of continua. In addition, there is a near degeneracy in energy of the $3d$ and $4s$ orbitals, which results in strong configuration interactions of the type $(3d,4s)^N$ with $3d^N \leftrightarrow 3d^{N-1}4s \leftrightarrow 3d^{N-2}4s^2$. The difficulties in the theoretical interpretation of the spectra have their counterparts in the experimental difficulties with the high temperatures required for the evaporation and the chemical aggressiveness of the liquid metals. The high temperatures also cause the thermal population of several initial states, which increases the number of transitions to be considered.

In this paper, we present the spectra of singly and doubly charged photoions of the elements Fe, Co, and Ni in the region of 50–80 eV. For the interpretation of the spectra we have calculated the respective photoionization cross sections starting from the thermally populated fine-structure states. Special emphasis will be placed on the origin of doubly charged photoions.

II. EXPERIMENT

The experiments were performed with the atomic-beam technique and the time-of-flight method for the detection of singly and doubly charged photoions. For the evaporation of the metals we used Al_2O_3 crucibles to avoid the direct contact of the molten metals with the molybdenum or tantalum furnaces that were heated by electron impact. The necessary temperatures for the three elements Fe, Co, and Ni were of the order of 1800 K to obtain a particle density of about $10^{11}/cm^3$ in the interaction region of atomic and photon beam. For the excitation of the atoms the monchromatized synchrotron radiation of the electron storage ring BESSY in Berlin was used. The resulting photoions were extracted by short electric pulses (120 V, 3-μs width, 17-kHz repetition rate) from the interaction region into a field-free drift tube after which they were detected by microchannel plates yielding the stop signals for the time-of-flight measurement. Electric fields between the atomic-beam source and the interaction region were applied to clean the beam from the large amount of ions that are produced by the evaporation process at such high temperatures and that would result in a nontolerable background of the photoion signals.

III. RESULTS

A. Fe

The experimental results of the photoion yield spectra of singly and doubly charged Fe ions in the region between 50 and 70 eV are shown in the lower part of Fig. 1. The main features in the Fe^+ signal are two broad resonances centered at 53.5 and 56.2 eV in good agreement with the results (53.3 and 56.1 eV, respectively) of the absorption measurements [2]. The same resonances are observed for the Fe^{2+} signal with a ratio of Fe^{2+}: $Fe^+ = 0.20(2)$ in the region of the reso-

*Present address: Max-Planck-Institut für Radioastronomie, D-53121 Bonn, Federal Republic of Germany.

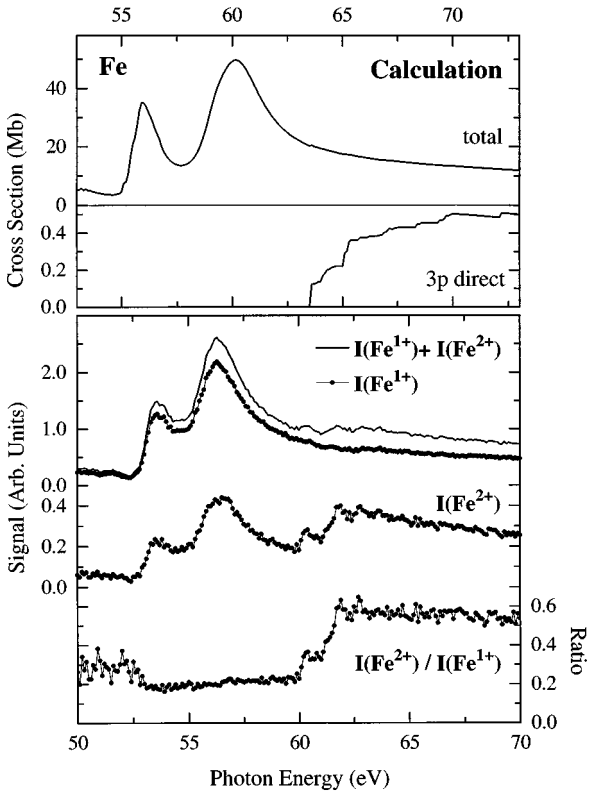

FIG. 1. Lower part: Photoion yield spectra of Fe in the region of the $3p$ excitation and ionization between 50 and 70 eV. Upper part: Calculated cross section for $3d,4s$, and $3p$ photoionization of the five initial states Fe $3d^6 4s^2\ ^5D$ weighted according to their thermal population at 1800 K. The $3p$ ionization is separately drawn for the discussion of the Fe^{2+} signal (see text). Note that the energy scale of the upper part is shifted.

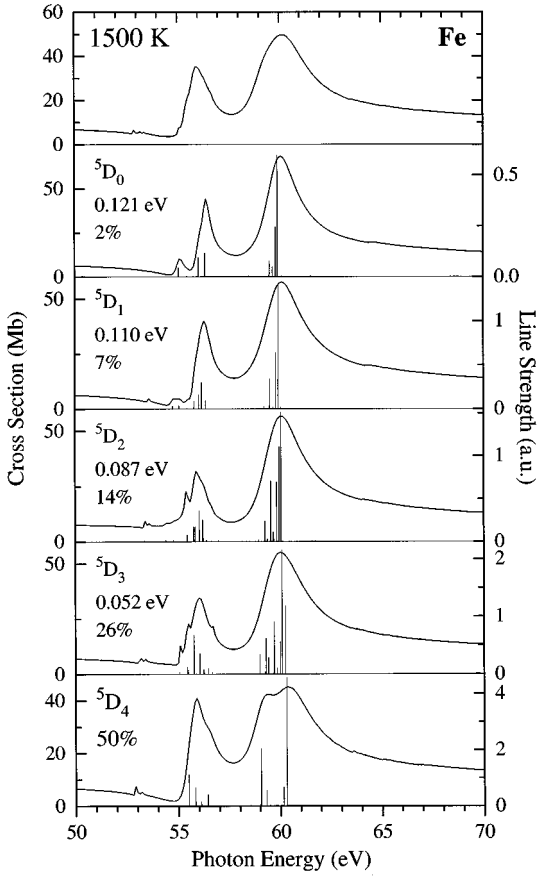

FIG. 2. Calculated cross section for $3d,4s$, and $3p$ photoionization of the five initial states Fe $3d^6 4s^2\ ^5D$. The vertical bars represent the line strength of the discrete transitions. The sum of the individual fine-structure contributions weighted according to the thermal population at 1800 K is given on top in Figs. 1 and 2.

nances between 53 and 60 eV. Below this region the ratio amounts 0.3(1), above 60 eV it increases in steps to 0.6(1) at 62 eV.

For an analysis of these signals we have calculated the $3d,4s$, and $3p$ photoionization cross section in the region of the $3p$ resonances. The calculations were performed in the framework of the Mies formalism [4]. In this formalism the Fano theory of isolated resonances interacting with many continua is extended to include the interaction of many resonances with many continua. In the Fano theory the width of a resonance Γ_n is defined as the sum of all its partial widths $\Gamma_{n,\beta}$ into the set of open channels $\{\beta\}$. When the width of adjacent resonances, however, begins to approach or exceed the spacings, the overlapping of resonances must be considered. For resonances that are coupled to different channels β, their shapes merely superimpose. For resonances that are coupled to the same channels, however, profound interference effects can exist. These effects are introduced by the nonvanishing off-diagonal elements of an ''overlap matrix'' between the continua to which neighboring states are coupled.

Configuration interaction of the type $(3d,4s)^N$ was taken into account by the configurations $3p^6 3d^6 4s^2 \leftrightarrow 3p^6 3d^7 4s \leftrightarrow 3p^6 3d^8$ for the initial states and $3p^5 3d^7 4s^2 \leftrightarrow 3p^5 3d^8 4s \leftrightarrow 3p^5 3d^9$ for the excited states. The continua were restricted to the configurations $3p^6(3d,4s)^7\varepsilon(p,f)$ for the $3d$ and $4s$ ionizations and to $3p^5(3d,4s)^8\varepsilon(s,d)$ for the $3p$ ionization.

At a temperature of about 1800 K, which was used for the production of the atomic beam of Fe the population of the initial states is concentrated in the five fine-structure states $3d^6 4s^2\ ^5D$ (0–0.12 eV) [3] with approximately 50% in the ground state $^5D_4$, 26% in the $^5D_3$, 14% in the $^5D_1$, 7% in $^5D_1$, and 2% in the $^5D_0$. The calculated photoionization cross sections of these five fine-structure states ^5D_J are shown in Fig. 2. These cross sections are weighted according to their thermal population at 1800 K resulting in the final curve on top of Figs. 1 and 2.

From a comparison of this final curve with the experimental results in Fig. 1 one can see that the main features with the two broad resonances are well reproduced although the positions and the distance of these maxima in this *ab initio* calculation are shifted to higher energies. The large number of individual resonances makes it impractical to list all transitions. We, therefore, have plotted the line strengths of the transitions as vertical bars below the cross sections. Although the line strengths usually can only be used in combination with the widths and asymmetry parameters of the resonances for an evaluation of the individual contributions to the signal, it is sufficient here to consider their values for a rough estimation of the relative importance of the different transitions.

The strongest transitions may be used for a tentative assignment of the resonances although one has to bear in mind that especially in the excited states there are strong deviations from *LS* coupling and the *LS* notation is only used for convenience describing the largest component in this representation. With this restriction the following assignment can be made: The first resonance at the experimental position of 53.5 eV is mainly caused by ^5F transitions and the second resonance at 56.2 eV by ^5P and ^5D transitions. In Ref. [2] the ^5P transitions are related to the first resonance, but we believe that the good agreement of experimental results and theoretical calculations support the ^5P and ^5D assignment to the second resonance. Because of configuration mixing of the type $(3d,4s)^N$ similar restrictions as for the *LS* representation hold for the notation of the configurations. Nevertheless, one can say that for the ^5F and ^5D transitions the main contributions are due to transitions $3p^6 3d^6 4s^2 \rightarrow 3p^5 3d^7 4s^2$, whereas for the ^5P transitions strong mixing between $3p^5 3d^7 4s^2$ and $3p^5 3d^8 4s$ occurs.

For the discussion of the individual Fe^+ and Fe^{2+} signals one has to consider the different decay routes. Photoelectron spectra [2] show that in this energy range there are seven main photoelectron lines that can be assigned to the corresponding Fe^+ states $(3d,4s)^7 LS$ as $3d^6 4s\ ^6D,^4D$, and $3d^5 4s^2\ ^6S,^4G,^4P,^4D,^4F$ with binding energies between 8 and 17 eV. These states cannot decay to Fe^{2+} (24.1 eV) so the final products in these decay routes are singly charged photoions. The Fe^{2+} signal below the $3p$ threshold, therefore, must be connected with other processes: (a) resonant or nonresonant double photoionization with the simultaneous emission of two electrons, which by sharing the remaining energy give rise to a continuous background in the photoelectron spectra or (b) the stepwise process by the decay of the highly excited Fe states into Fe^+ states above 24.1 eV with the subsequent Auger decay into Fe^{2+}. This process should be detected in the photoelectron spectra by the occurrence of satellite lines above 24.1 eV binding energy. As the photoelectron spectra [2] do not exhibit such satellite lines one may conclude that below the $3p$ threshold only process (a) is responsible for the production of Fe^{2+}. The large number of states connected with the coupling properties of the remaining $3d$ electrons and the widths of these states, however, can lead to a quasicontinuous character of the satellite structure in process (b) so that no clear distinction between the two processes can be made.

Above the $3p$ threshold direct $3p$ ionization with the subsequent Auger decay of the Fe^+ $3p^{-1}$states to Fe^{2+} is possible. One, therefore, expects an increase of the Fe^{2+} signal above this threshold. The lowest $3p$ ionization limit was estimated at 63.7(5) eV [5] and also the $3p$ ionization cross section of our calculation starts at 63.5 eV (Fig. 1 upper part) although in this *ab initio* calculation the energy positions as in the case of the resonances may be shifted. We, therefore, cannot decide whether the stepwise increase of the Fe^{2+} signal starting at 60 eV is connected with the successive opening of different $3p^{-1}$ channels or with the increasing tendency of resonances below the $3p$ threshold to decay to Fe^{2+}.

B. Co

The photoion yield spectra of Co^+ and Co^{2+} in the region of 52.5–75 eV are shown in Fig. 3. The main features of the

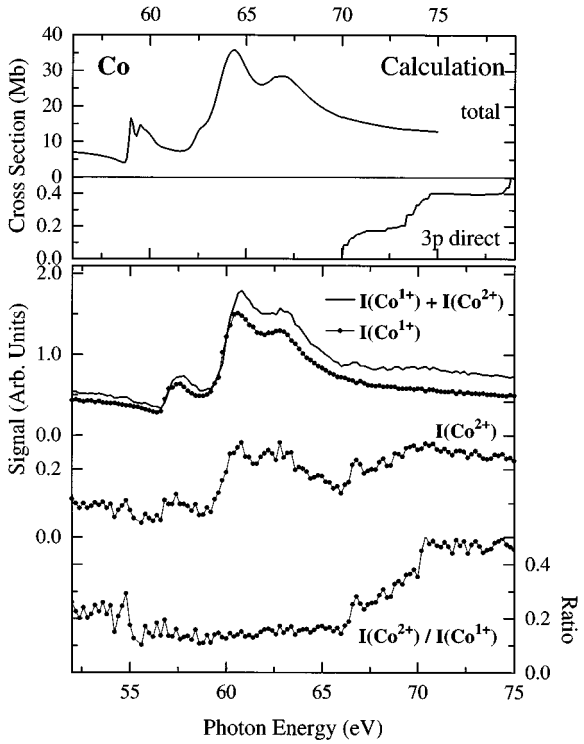

FIG. 3. Lower part: Photoion yield spectra of Co in the region of the $3p$ excitation and ionization between 53 and 75 eV. Upper part: Calculated cross section for $3d,4s$, and $3p$ photoionization of the five initial states Co $3d^7 4s^2\ ^4F$ weighted according to their thermal population at 1800 K. The $3p$ ionization is separately drawn for the discussion of the Co^{2+} signal (see text). Note that the energy scale of the upper part is shifted.

Co^+ signal are three resonances centered at 57.4, 60.6, and 62.7 eV in good agreement with the results (57.6, 60.4, 62.7 eV) of the absorption measurements [2]. The same resonances can be seen in the Co^{2+} signal with a ratio of Co^{2+}: $Co^+ = 0.15(3)$. This ratio increases above 66 eV in steps to 0.46(5) at 70 eV.

Similar to the Fe signals we have analyzed the Co signal by the calculation of the $3d,4s$, and $3p$ photoionization cross sections. At the temperature of 1800 K the population of the initial states is concentrated in the four fine-structure states $3d^7 4s^2\ ^4F$ (0–0.22 eV) [3] with approximately 59% in the ground state $^4F_{9/2}$, 24% in the $^4F_{7/2}$, 11% in the $^4F_{5/2}$ and 6% in the $^4F_{3/2}$. The continua were restricted to the configurations $3p^6(3d,4s)^8\varepsilon(p,f)$ for the $3d$ and $4s$ ionization and to $3p^5(3d,4s)^9\varepsilon(s,d)$ for the $3p$ ionization. The resonances are due to the discrete transitions $3p^6(3d,4s)^9 \rightarrow 3p^5(3d,4s)^{10}$. The calculated photoionization cross sections of the four fine-structure states ^4F_J in the region of 50–75 eV are depicted in Fig. 4.

The individual fine-structure contributions are weighted according to the thermal population at 1800 K with the result of the final curve on top of Figs. 3 and 4. The comparison of this final curve with the experimental results in the lower part of Fig. 3 shows good qualitative agreement with the main features of the three groups of resonances although the positions of these resonances in the *ab initio* calculation are shifted to higher energies.

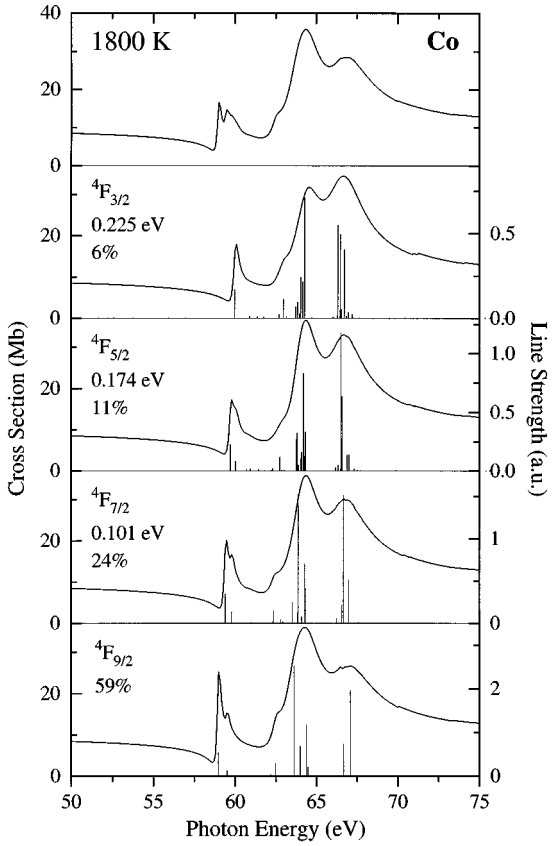

FIG. 4. Calculated cross section for $3d,4s$, and $3p$ photoionization of the five initial states Co $3d^7 4s^2\ ^4F$. The vertical bars represent the line strength of the discrete transitions. The sum of the individual fine-structure contributions weighted according to the thermal population at 1800 K is given on top in Figs. 3 and 4.

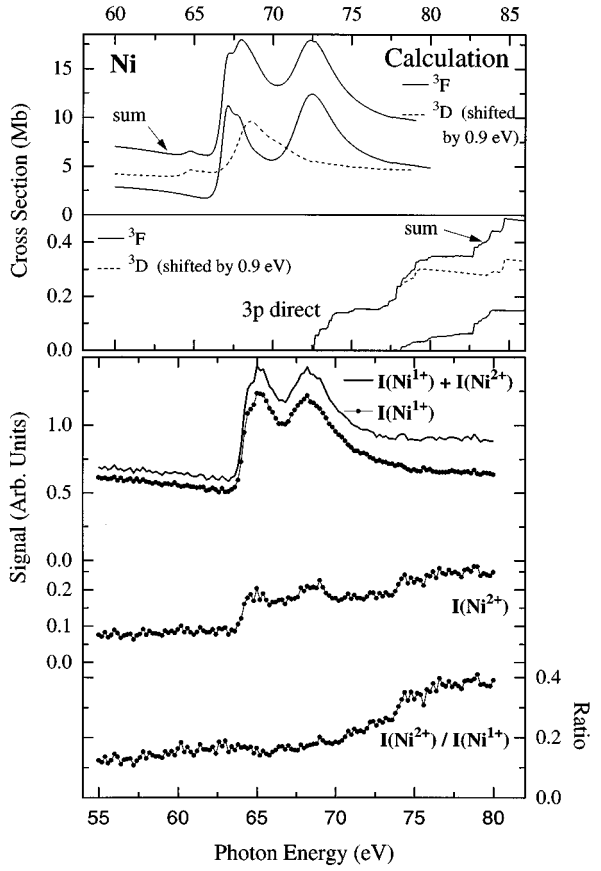

FIG. 5. Lower part: Photoion yield spectra of Ni in the region of the $3p$ excitation/ionization between 55 and 80 eV. Upper part: Calculated cross section for $3d,4s$, and $3p$ photoionization of the six initial states Ni $3d^8 4s^2\ ^3F$ and $3d^9 4s\ ^3D$ weighted according to their thermal populations at 1800 K. The $3p$ ionization of both configurations is separately drawn for the discussion of the Ni^{2+} signal (see text). Note that the energy scale of the upper part is shifted.

The vertical bars indicate the line strength of the discrete transitions. With the same reservation with respect to the *LS* and configuration notation as in the case of Fe one can use the strongest transitions for a tentative assignment of the resonances: The resonance at the experimental position of 57.4 eV is mainly caused by ^4G transitions, the resonance at 60.6 eV by ^4F transitions, and the resonance at 62.7 eV by ^4D transitions. The ^4G and ^4F transitions are mainly due to $3p^6 3d^7 4s^2 \rightarrow 3p^5 3d^8 4s^2$, whereas for the ^4D transitions strong mixing between $3p^5 3d^8 4s^2$ and $3p^5 3d^9 4s$ occurs.

The discussion of the Co^{2+} signal raises the same problems as for the Fe^{2+} signal. Below the *3p* threshold direct double ionization to Co^{2+} (24.9 eV) or stepwise decay of highly excited Co states into Co^+ states above 24.9 eV with subsequent Auger decay into Co^{2+} should be responsible for the Co^{2+} signal. The distinction between these two processes by the detection of a continuous electron distribution or a discrete satellite structure above 24.9-eV binding energy, however, cannot be made at present by the experimental data of the photoelectron spectra [5]. Above the $3p$ threshold the possibility of direct $3p$ ionization with the subsequent Auger decay of $Co^{2+}\ 3p^{-1}$ states to Co^{2+} should increase the Co^{2+} signal. The $3p$ ionization limit was estimated at 70(1) eV [5] and the calculated onset of the direct $3p$ ionization is also at 70 eV (see Fig. 3), although one has to keep in mind that in these *ab initio* calculations this energy position may be shifted as in the case of the resonances. Similar to the case of Fe^{2+} we cannot decide whether the increase of the Co^{2+} signal above 66 eV is connected with the successive opening of the different $3p^{-1}$ channels in this region or with $3p$ resonances which predominantly decay to Co^{2+}.

C. Ni

The photoion yield spectra of Ni^+ and Ni^{2+} in the region of 55–80 eV are shown in the lower part of Fig. 5. There is one resonance at 65.0 eV with a shoulder at 64.6 eV and a second resonance at 68.2 eV in good agreement with the results (65.0, 64.2, 67.7 eV) of the absorption measurements [2]. In contrast to Fe and Co the ratio of N^{2+}:Ni^+ does not exhibit a constant value in the region of the resonances but slowly rises from a value of 0.15(3) at about 68 eV to 0.38(4) at 80 eV.

The analysis of the Ni signals is complicated by the fact that at 1800 K the initial states of both configurations $3d^8 4s^2\ ^3$F (0–0.27 eV) and $3d^9 4s\ ^3D$ (0.023–0.21 eV) [3] are populated: $3d^8 4s^2\ ^3F_4$ (42%), $^3F_3$ (11%), $^3F_2$ (4%), and $3d^9 4s^2\ ^3D_3$ (28%), $^3D_2$ (11%), $^3D_1$ (4%). The important difference of both configurations is the unfilled $4s$ subshell

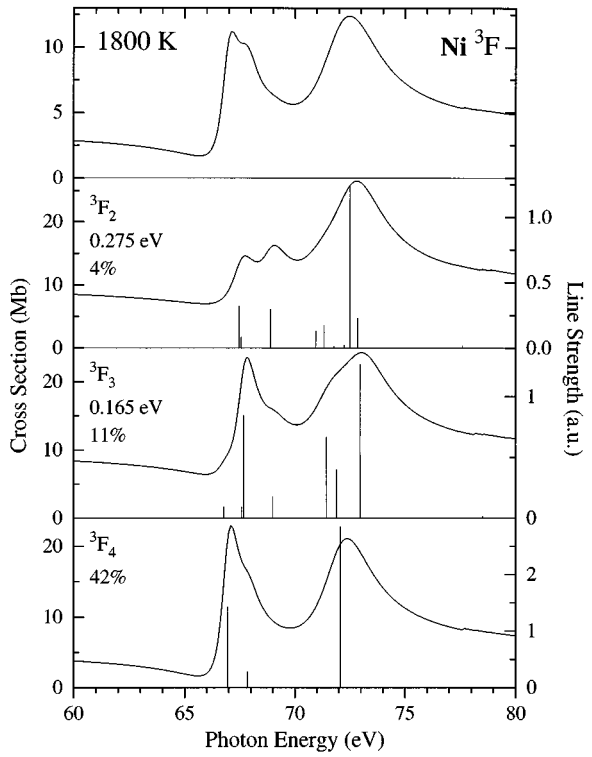

FIG. 6. Calculated cross section for $3d,4s$, and $3p$ photoionization of the three initial states Ni $3d^8 4s^2\ ^3F$. The vertical bars represent the line strength of the discrete transitions. The sum of the individual fine-structure contributions weighted according to the thermal population at 1800 K is given on top of Figs. 5 and 6.

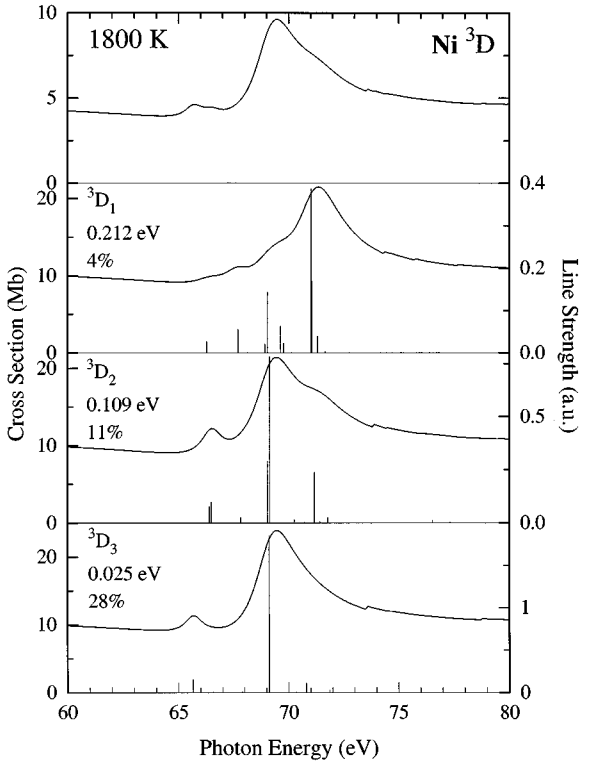

FIG. 7. Calculated cross section for $3d,4s$, and $3p$ photoionization of the three initial states Ni $3d^9 4s\ ^3D$. The vertical bars represent the line strength of the discrete transitions. The sum of the individual fine-structure contributions weighted according to the thermal population at 1800 K is given on top of Figs. 5 and 6.

of $3d^9 4s$, which enables transitions of the type $3p \rightarrow 4s$. Whereas for the configuration $3d^8 4s^2$ the resonances are mainly due to the transitions $3d^8 4s^2 \rightarrow 3p^5 3d^9 4s^2$, in case of $3d^9 4s$ one has to consider both types of transitions: $3d^9 4s \rightarrow 3p^5 3d^{10} 4s$ and $3d^9 4s \rightarrow 3p^5 3d^9 4s^2$.

The calculation of the $3d,4s$, and $3p$ photoionization cross section was performed in the same way as for Fe and Co. The results of the different fine-structure levels $3d^8 4s^2\ ^3F$ and $3d^9 4s\ ^3D$ are given in Figs. 6 and 7 with the sum weighted according to the thermal population on top of each figure. The vertical bars represent the line strength of the discrete transitions. With the same reservation the *LS* and configuration notation because of deviations from *LS* coupling and of configuration interaction one can use the strongest transitions for a tentative assignment of the resonances:

(a) Starting from the initial states $3d^8 4s^2\ ^3F$ the first resonance is mainly due to transitions into $3p^5 3d^9 4s^2\ ^3F$ and the second resonance to transitions into $3p^5 3d^9 4s^2\ ^3D$.

(b) Starting from the initial states $3d^9 4s\ ^3D$ the dominant resonance is mainly due to transitions into $3p^5 3d^{10} 4s\ ^3P$, whereas the small features on the low-energy side are due to transitions into $3p^5 3d^9 4s^2\ ^3F$.

There is good qualitative agreement between the sum of the calculated cross sections from both initial configurations with the photoion signals if one shifts the contribution of the initial state $3d^9 4s\ ^3D$ (top of Fig. 7) relative to that of $3d^8 4s^2\ ^3F$ (top of Fig. 6) by an amount of 0.9 eV so that the dominant resonance of the $3d^9 4s\ ^3D$ contribution nearly coincides with the first resonance of the $3d^8 4s^2\ ^3F$ contribution. (This shifting is justified because the mismatch of energy positions of states form different configurations is a general problem in the Hartree-Fock calculation.) The resonance at the experimental position of 65.0 eV with the shoulder at 64.6 eV, therefore, can be attributed to transitions $3d^8 4s^2\ ^3F \rightarrow 3p^5 3d^9 4s^2\ ^3F$ and $3d^9 4s\ ^3D \rightarrow 3p^5 3d^{10} 4s\ ^3P$ with the distinction that the shoulder at the low-energy side at 64.6 eV is more due to the $^3F \rightarrow {}^3F$ transitions. The second resonance at 68.2 eV can be mainly attributed to transitions $3d^8 4s^2\ ^3F \rightarrow 3p^5 3d^9 4s^2\ ^3D$.

For the discussion of the Ni^{2+} signal one can consider the ratio Ni^{2+}: Ni^+ (lower part of Fig. 5), which in the region of the first resonance with Ni^{2+}: $Ni^+ = 0.15(3)$ is of the same order as that of Fe^{2+}: Fe=0.20(3) and Co^{2+}: Co=0.15(3) in the region of their resonances, but which in contrast to Fe and Co already starts to increase in the region of the second resonance at about 69 eV. If we assume that this increase is connected in some way with the $3p$ threshold we have to consider both initial configurations $3d^8 4s^2$ and $3d^9 4s$. The upper part of Fig. 5 shows the calculated cross sections of the $3p$ ionization from the initial states $3d^8 4s^2\ ^3F$ (solid line) and $3d^9 4s\ ^3D$ (dashed line). One can see that the threshold of the $3p$ ionization from the initial states $3d^9 4s\ ^3D$ is, indeed, in the region of the second resonance, which is due to discrete transitions from the initial states $3d^8 4s^2\ ^3F$. There-

fore, it sounds plausible to associate the increase of Ni^{2+}: Ni^{+} at the region of the second resonance with the configuration $3d^9 4s\ ^3D$. With respect to the absolute positions of the calculated thresholds 73.5 eV ($3d^9 4s\ ^3D$) and 78 eV ($3d^8 4s^2\ ^3F$) and the estimated value 78.8(2.0) eV [5] one has to bear in mind that as in the case of Fe and Co the positions in this *ab initio* calculation may be shifted.

Summarizing the results, we have observed the spectra of singly and doubly charged photoions of the elements Fe, Co, and Ni in the region of the $3p$ excitation. The sums of the X^+ and X^{2+} signals (the X^{3+} signal was negligible) are in good agreement with the absorption measurements [2]. Decay by fluorescence, therefore, is only a minor effect in this region. There is, however, quite a remarkable contribution of doubly charged photoions in the order of 10%–50%. For the interpretation of the spectra we have calculated the photoionization cross section starting from the thermally populated fine-structure levels (in the case of Ni from the two configurations).

ACKNOWLEDGMENTS

We are thankful for the financial support from the Bundesminister für Forschung und Technologie (BMFT) and from the Deutsche Forschungsgemeinschaft (DFG). This work was carried out within the framework of the EU HC&M Programme.

[1] B. Sonntag and P. Zimmermann, Rep. Prog. Phys. **55**, 911 (1992).

[2] M. Meyer, Th. Prescher, E. v. Raven, M. Richter, E. Schmidt, B. Sonntag, and H.-E. Wetzel, Z. Phys. D **2**, 347 (1986).

[3] C. E. Moore, *Atomic Energy Levels*, Natl. Bur. Stand. (U.S.) Circ. No. 467 (U.S. GPO, Washington, DC, 1971), Vol. II.

[4] F. H. Mies, Phys. Rev. **175**, 164 (1968).

[5] E. Schmidt, H. Schröder, B. Sonntag, H. Voss, H.-E. Wetzel, J. Phys. B **17**, 707 (1984).